[SSC24-WI-08]

# Engineering Model Development of LunaCube: 6U Dual-satellite Lunar Navigation and Communication System

Hirotaka Sekine, Kazuki Toma, Takeshi Matsumoto, Shinichi Nakasuka
The University of Tokyo
7-3-1 Hongo, Bunkyo-ku, 113-8656, Tokyo, Japan; +81-3-5841-6608
sekine@space.t.u-tokyo.ac.jp

Toshiki Tanaka
University of Houston
306 Technology 2 Bldg., Calhoun Road, Houston, 77004, TX, USA
ttanaka@uh.edu

Takuji Ebinuma, Rion Sobukawa
Chubu University
1200, Matsumoto-cho, 487-8501, Kasugai, Aichi, Japan; +81-568-51-9320
ebinuma@isc.chubu.ac.jp

Yoshihide Aoyanagi
University of Fukui
3-9-1, Bunkyo, 910-8507, Fukui, Japan; +81-776-27-8990
aoyanagi@u-fukui.ac.jp

## ABSTRACT

Lunar navigation and communication satellite systems are now recognized as important infrastructure for more efficient lunar exploration. While establishing a full constellation system will take several more years, lunar surface explorations are already becoming more active. To address the immediate demand for positioning and communication relay, especially in the South Pole region, a nimble technology demonstration mission named Lunar Navigation CubeSat (LunaCube) has been proposed. Following the completion of preliminary design in 2021 and detailed design in 2022, the engineering model was developed in 2023. This paper presents updated orbit analysis that considers trade-off between orbit maintenance costs and positioning accuracy in low lunar orbits. Additionally, this paper details the development results of engineering models for components, such as the lunar navigation transmitter and the store-and-forward radio. It also summarizes the results of the system's environmental tests.

## INTRODUCTION

To date, a significant number of lunar exploration missions are under development across both governmental and commercial sectors. Many of these missions focus on scientific observations or resource exploration on the lunar surface. As a result, a precise navigation system localized to the Moon will be required for the lunar surface vehicles, such as rovers.

A multi-user navigation platform, such as a global lunar navigation satellite system (LNSS), is considered key to supporting a wide range of on-surface transportation activities simultaneously. For this purpose, several global LNSS missions, comprising constellations of navigation satellites around the Moon, have been conceptualized, including *LCRNS* by NASA,[1] *Moonlight* by ESA,[2] and *LNSS* by JAXA.[3] While it is expected that their services will be fully functional in the late 2020s, many missions are set to begin on-surface exploration even before then.

To address the immediate demand for positioning and communication relay especially in the South Pole region, a nimble technology demonstration mission named Lunar Navigation CubeSat (LunaCube)[4] has been proposed. This mission, funded by the Japanese Ministry of Education, Culture, Sports, Science, and Technology, has progressed through preliminary design in 2021, detailed de-

sign in 2022, and the development of an engineering model in 2023.

The LunaCube is a dual-satellite lunar navigation system that employs the multi-epoch double-differenced pseudorange observation (MDPO) algorithm.[5] The MDPO process involves collecting pseudorange measurements between two lunar orbiters and both the user and surface reference receivers. Through the double-difference observation process, the influences of satellite orbit determination (OD) errors and satellite clock offset on user positioning accuracy are significantly eliminated. This reduces the reliance on high-standard onboard clocks that require high power. Consequently, it enables the use of small-sized satellites, achieving a 50-meter user positioning accuracy with just a one-minute observation by placing two 6U satellites in a low lunar orbit (LLO).

Overall, the distinct advantages of this approach include the use of small-sized satellites, a short observation period, and accuracy sufficient for many mission applications. Thus, this navigation option is not only easy to establish and useful for supporting early-phase surface missions, but it can also provide additional regional coverage and serve as a backup for other global navigation systems.

One of the primary design considerations for the LunaCube satellite is their orbits because the relative position of the two satellites has a huge impact on the positioning accuracy in the MDPO algorithm.[5] Several groups have studied positioning algorithms that reduce the number of satellites required for positioning services.[5–9] However, to the best of our knowledge, no research has been conducted on orbit optimization specifically for the dual-satellite LNSS.

Previous research on lunar orbit design and optimization have predominantly focused on higher orbits to increase service coverage and reduce orbit maintenance costs. Examples include halo orbits,[10–16] frozen orbits,[12,16–19] distant retrograde orbits,[11,14,16] and inclined circular orbits.[12,20–24] However, these approaches are not directly applicable in LLO where the gravity anomaly has a substantial impact on satellites' orbits.

In terms of the astrodynamics in LLO, SELenological and ENgineering Explorer (SELENE)[25] and Lunar Reconnaissance Orbiter (LRO)[26] required a significant amount of Delta-V to exploit the evolution of eccentricity $e$ and the argument of perilune $\omega$. On the other hand, Korea Pathfinder Lunar Orbiter (KPLO) proposed an orbit maintenance method called scheduled circularization control (SCC),[27] successfully reducing Delta-V by using a simple Hohmann transfer. The SCC method is applied to this specific mission, with its scope expanded to include relative position control.

The detailed design results of the LunaCube has been published earlier. This paper provides incremental updates including the orbit analysis and the progress of the engineering model development.

## MISSION OVERVIEW

The dual-satellite positioning algorithm used for LunaCube is the MDPO.[5] The MDPO utilizes double-differenced observation using a reference station on the lunar surface. It eliminates the clock errors of the rover, the reference station, and the satellites. Therefore, the clock stability requirement is relaxed for both satellites and rovers, enabling the use of small-sized satellites for navigation service, and it is suitable for the early phase rovers. The double-differenced observation also reduces user position estimation errors caused by uncertainties in satellite OD. This is critical in reducing dependence on ground stations during mission operations. It is worth noting that pseudorange measurements observed at the reference station are to be transferred to the rovers for double-difference observation. Therefore, LunaCube satellites carry not only lunar navigation systems (LNS) transmitters but also store-and-forward (S&F) radios. It is also worth noting that the MDPO is a relative navigation algorithm, and the position of the reference station should be pre-known.

Furthermore, the MDPO utilizes multi-epoch observations to reduce the minimum number of satellites required for the navigation service from four to two. To estimate the three-dimensional position of rovers, at least three epoch observations are required. When the digital elevation model (DEM) of the lunar surface is available during the estimation process, the required number of observations decreases from three to two. In this paper, positioning is performed based on two observations taken at 30-second intervals within the first minute, followed by the assumption that the rover moves during the next 30 seconds. This 90-second process is repeated during the approximately 10 minutes when both satellites are simultaneously visible from the rover.

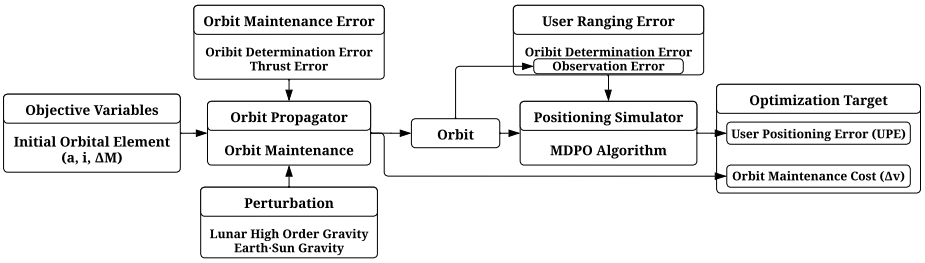


**Figure 1: Overview of orbit propagator and positioning simulator.**

## ORBIT SELECTION

### *Overview*

For lunar navigation in the South Pole region, placing the apolune in the Moon's southern hemisphere would maximize visibility of that area. However, in elliptical orbits, the satellite's angular velocity is low near the apolune when viewed from the lunar surface, leading to poor dispersion of satellite positions over time.

This limitation is particularly critical for the MDPO algorithm, which relies on significant satellite movement between multi-epoch observations to enhance positioning accuracy. In contrast, a circular orbit ensures consistent satellite dispersion over time from the South Pole.

Therefore, a low lunar circular orbit is selected for the LunaCube. LLO is chosen, leveraging the limited power of a 6U CubeSat to provide a navigation service for the lunar surface.

### *Models and Methods*

In this research, two primary requirements derived from the LunaCube mission and systems design were considered: the amount of fuel to bring and the desired user positioning accuracy.

The MDPO algorithm requires continuous visibility of two satellites from the rover over a specific period for positioning. Thus, it is essential to maintain a low value for the mean anomaly difference, $\Delta M$, between the two satellites through orbit maintenance. The total fuel required for the mission duration must be minimized as the 6U CubeSat has a limited fuel capacity. In this research, the total delta-V required for the mission period is represented as $\Delta v$ and is used as the metric.

The relative positions of the two satellites vary, altering their visibility from the user's perspective. The geometric arrangement of satellites is indicated by the dilution of precision (DOP), and DOP determines the user positioning accuracy. The LunaCube mission requires a horizontal user positioning accuracy of less than several tens of meters. This study employs the user positioning error (UPE) as the metric to meet this requirement. The UPE represents the horizontal Euclidean distance averaged over the entire mission duration and is expressed as 2drms (twice the distance root mean square). The expression for the DOP and UPE in the MDPO algorithm is provided in our previous paper.[5]

Since $\Delta v$ and UPE have a trade-off relationship, they must be optimized simultaneously. A lower orbital altitude improves signal reception and UPE, whereas a higher orbital altitude decreases the effect of the higher-order gravity of the Moon that dominates in LLO, thereby reducing the $\Delta v$ for orbit maintenance.

A performance index is defined to balance out two trade-off metrics. The performance index $J$ is described as

$$\min_{\mathrm{OE}} \quad J = k_a \Delta v + k_b \mathrm{UPE} \tag{1}$$

where $k_a$ and $k_b$ are user-set constants to weight $\Delta v$ and UPE. In this study, the aim is to optimize the dual satellites' orbit elements (OE). When inserting into the same circular orbit, the three OE considered are semi-major axis $a$, the inclination $i$, and $\Delta M$.

Figure 1 shows the relationship between the optimization target and the objective variables. The SCC method is extended to control the relative position between two satellites. In LLO, $e$ and $a$ vary due to the Moon's rotation period. Therefore, the SCC method aims to revert the satellite's orbit to circular after every lunar rotation period. In the MDPO algorithm, it is crucial to maintain the relative position of the dual satellites. Thus, the target semi-major axis $a_{target}$ for each orbit maintenance is adjusted to maintain the phase difference between

**Table 1: Sources of error for the numerical simulation ($1\sigma$).**

| Error | Type | Value | Unit |
|---|---|---|---|
| Thrust Error Magnitude $\Delta v_{mag}$ | white noise | 1.67 | % |
| Thrust Error Direction $\Delta v_{dir}$ | white noise | 3.33 | deg |
| OD Error $\Delta X^s{}_{OD}$ | white noise | (3.3, 33.3, 33.3) | m |
| (Radial, Along, Cross) | systematic noise | (20, 200, 200) | m |
| Observation Error $\eta$ | white noise | 0.5 | m |
| | bias noise | 0 | m |
| Time Tag Error $\Delta X^s{}_{TT}$ | bias noise | 1 | ms |
| | random walk | 1e-8 | ms/min |
| DEM Error | white noise | 10 | m |
| | systematic noise | 5 | m |
| Range measurement resolution | | 0.4 | m |

the two satellites close to the nominal value $\Delta M$.

### *Numerical Simulation Settings*

A simulator incorporating precise orbital dynamics and perturbations for numerical optimization has been developed. Orbit propagation was performed over the mission period based on the initial OE while considering thrust and OD errors. The mission period was set for one year. In the orbit propagator, the Orbit Determination Toolbox developed by NASA Goddard Space Flight Center was used. The GL0660B gravity model up to the 20th degree and order was used for the Moon. The third body attraction of the Sun and the Earth was also considered.

The weight parameters in Eq. 1 were set to $k_a = 1/24.5$ and $k_b = 1/100$ based on the $\Delta v$ budget of DVT and the target positioning accuracy in the LunaCube mission. The initial rover and lander positions are at the South Pole, and rover moves 3.75 m between two positioning. The rover's movement direction is assumed to change randomly by selecting from $-\frac{\pi}{3}, 0$, or $\frac{\pi}{3}$ relative to its previous direction. The minimum elevation angle was set at 5 degrees to prohibit detrimental observations.

Table 1 summarizes the other user-set variables used in the numerical simulations. The thrust $\Delta v_{mag}, \Delta v_{dir}$, and OD $\Delta X^s{}_{OD}$ errors were set based on the previous analysis[28] and the in-flight data.[29] It is important to note that the systematic noise of OD errors is derived from the satellite's navigation message and only affects positioning calculations. Observation errors $\eta$ consist of both white noise and bias noise. The white noise was set as 0.5 m/s. The main source of bias noise in $\eta$ is multipath, and on the lunar surface, multipath is primarily caused by reflections. By designing the antenna to avoid receiving signals from the lunar surface, multipath effects can be minimized, allowing the bias noise to be set to 0. Time tag error $\Delta X^s{}_{TT}$ and range measurement resolution values were set according to the previous study.[5]

This study compared 80 candidate orbits, considering different combinations of $h$, $i$, and $\Delta M$ as shown in Table 2. It is worth noting that $h$ can be calculated by subtracting the Moon's radius from $a$.

**Table 2: 80 candidate orbits for a grid search.**

| Parameter | Value | Unit |
|---|---|---|
| $h$ | 100, 200, ..., 500 | km |
| $i$ | 70, 75, 80, 85 | deg |
| $\Delta M$ | 5, 10, 15, 20 | deg |

### *Numerical Simulation Results*

Figure 3 shows UPE calculated for each orbit. Positioning was not performed when both the orbit $h$ and $i$ were low because the simultaneous visibility duration of the two satellites was less than the time needed for multiple observations. Figure 4 shows each orbit's performance index $J$.

Table 3 summarizes five orbits with the lowest performance index $J$ among the candidates. It has been confirmed that orbits with a small performance index $J$ typically have an $h$ of 200 or 300 km, a $\Delta v$ of approximately 7.3-11.5 m/s, and a UPE of around 16.4-32.8 m.

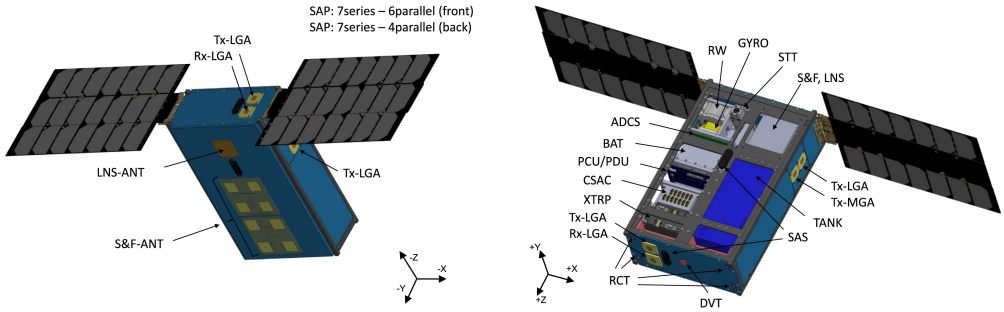


**Figure 2: Satellite overview.[4]**

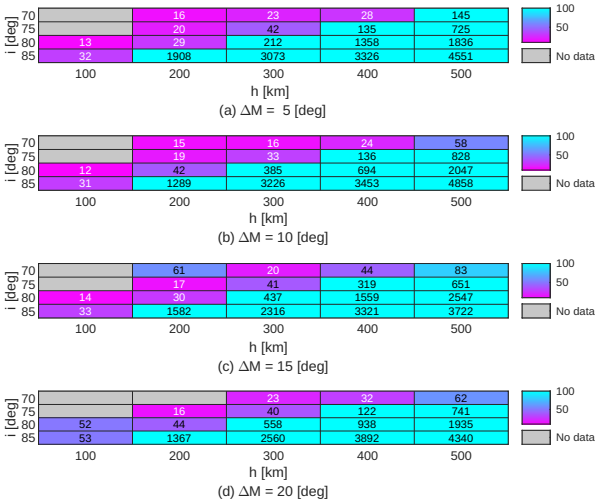


**Figure 3: UPE [m] calculated for each orbit.**

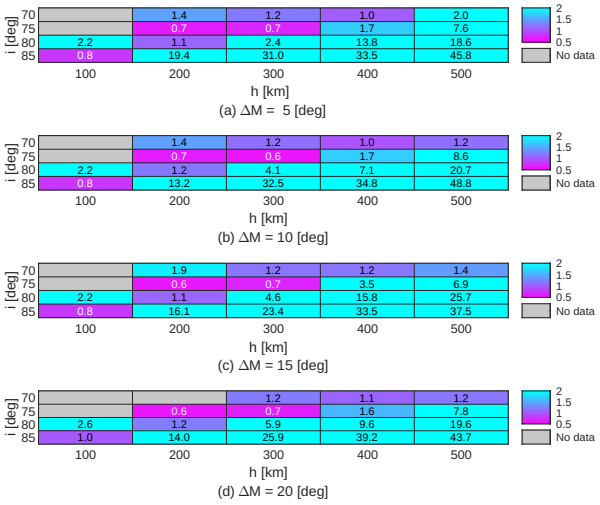


**Figure 4: The performance index J calculated for each orbit.**

**Table 3: Five orbits with the lowest performance index $J$ among the candidates.**

| $h$ [km] | $i$ [deg] | $\Delta M$ [deg] | $\Delta v$ [m/s] | UPE [m] | $J$ |
|---|---|---|---|---|---|
| 300 | 75 | 10 | 7.3 | 32.8 | 0.6 |
| 200 | 75 | 20 | 11.5 | 16.4 | 0.6 |
| 200 | 75 | 15 | 11.5 | 16.6 | 0.6 |

### *Discussion*

The numerical simulation results offer critical insights into the effects of each OE parameter. One key finding, shown in Figure 3, is that the positioning accuracy worsens with increasing values of $h$. As the satellite's altitude increases, the satellite's angular velocity as seen from the user decreases, which worsens the horizontal DOP. In this paper, the standard deviation of observation error is fixed. However, if the deterioration of the signal-to-noise ratio due to the increasing distance between the satellite and the user is considered, the degradation in positioning accuracy with higher satellite altitudes would be even more severe.

The results also underscore the importance of considering orbit maintenance costs when identifying optimal orbits. While orbits at an altitude of 100 km could be considered optimal based solely on UPE, their high orbit maintenance costs rule them out, as shown in Table 3.

Notably, the findings indicate that strict control of the absolute position of satellites is not essential for the LunaCube mission, which employs the MDPO algorithm. Even with orbits deviating slightly from the optimal in terms of $a$, $i$, or $\Delta M$, the UPE remains within several tens of meters and $\Delta v$ stays below 24.5 m/s, satisfying the LunaCube mission's requirements. The priority should be controlling the relative positions between satellites to maintain geometric dispersion from the lunar surface, which can be achieved with simple orbit maintenance expanded from SCC.

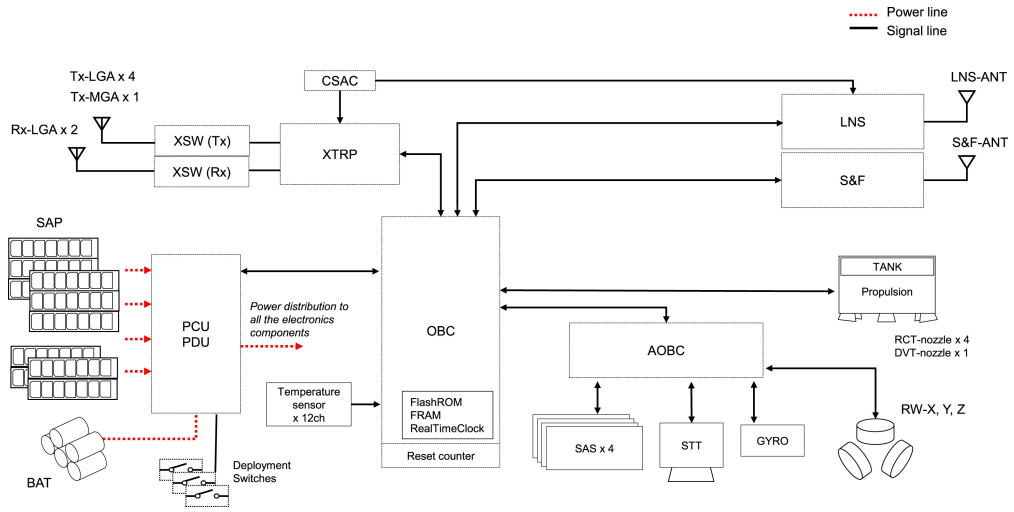


**Figure 5: Systems diagram.**[4]

## SPACECRAFT SYSTEM DESIGN AND ENGINEERING MODEL DEVELOPMENT

This section provides an overview of the system design as well as the engineering model test results, which are published for the first time.

### *System*

The overview of LunaCube is shown in Figure 2. Its size is $100 \times 226.3 \times 366$ mm$^3$ and its wet mass is less than 14 kg. The systems diagram is shown in Figure 5.

### *LNS Transmitter*

The LNS transmitter, based on software defined radio (SDR), allows for flexible adjustments to frequency and modulation methods, enabling compatibility with other global navigation systems in later phases. The design of the LNS transmitter was carried out with the assumption that the frequency of the lunar navigation signal would be in the S-band (2483.5-2500.0 MHz) as recommended by the Space Frequency Coordination Group. For the precise time synchronization required for the positioning signal, a Chip-Scale Atomic Clock (CSAC) is used.

The basic design of the positioning transmitter has been completed, and as shown in Figure 6, a prototype has been developed. The prototype has passed radiation tests, confirming functionality in cislunar environments. Additionally, it has undergone vibration testing (12.6 Grms, 80 seconds) and thermal vacuum testing (low temperature -10°C, high temperature +50°C), confirming its integrity.

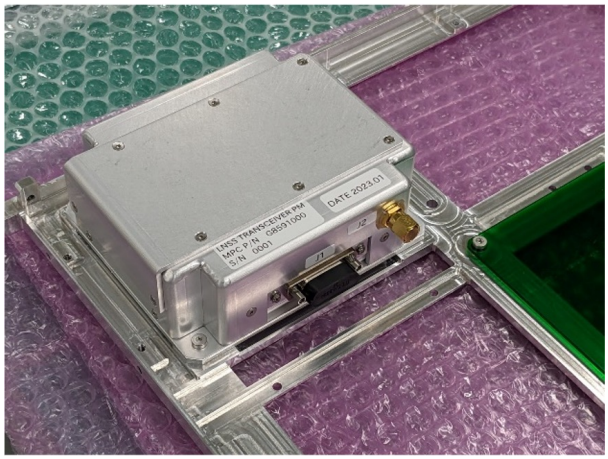

**Figure 6: Prototype of the LNS transmitter.**

### *Store-and-Forward Radio*

To provide a communication relay service for rovers and a reference station, a S&F radio, developed from the heritage of the LoRa module, is installed. This technology was previously employed in missions such as TRICOM-1R, launched in 2018, demonstrating the ability to receive signals on the satellite with just 8 mW of ground transmission power. The S&F radio has already completed the manufacturing of the engineering model and the antenna pattern testing, as shown in Figure 7.

**Figure 7: Engineering model of the store and forward radio.**

| Components | Specifications |
|---|---|
| RW | Momentum 30.6 mNms |
| | Max torque 2.3 mNm |
| STT | Cross-boresight accuracy 15 arcsec ($1\sigma$) |
| | Around boresight accuracy 90 arcsec ($1\sigma$) |
| SS | Field of view $\pm$ 60 degrees |
| | Accuracy $\leq$ 0.5 degrees |
| Gyro | Bias stability $<$ 0.3 degrees/h |
| | Angle random walk $<$ 0.15 degrees/$\sqrt{\text{h}}$ |
| | Range $>$ $\pm$ 200 degrees/s |

**Table 5: Propulsion system specification.**

| Specifications | DVT | RCT |
|---|---|---|
| Thrust level [mN] | 4.0 | 1.0 |
| Isp [s] | 70 | $>$ 50 |
| Fuel [g] | 500 | 400 |
| Cant angle [degrees] | 0 | 30 |

### *AOCS*

The ADCS consists of a star tracker (STT), four sun sensors (SSs), a gyroscope (GYRO), and three reaction wheels (RWs). They are selected to satisfy attitude determination and control requirements in all modes of operation and their specifications are summarized in Table 4.

The propulsion system uses water propellant resistojet thrusters, which are a customized product based on the AQUA ResIstojet propUlsion System (AQUARIUS).[30] It consists of one DVT for orbit maintenance and four RCTs for angular momentum management. The specifications of the propulsion system is summarized in Table 5. 500 g of water is allocated for orbit maintenance and it is enough for a two-year mission as shown in the previous section. 400 g of water is allocated for angular momentum management. Based on the disturbance torque calculation, accumulated angular momentum is estimated to be about 0.003 Nms/day. When the cant angle is 30 degrees, Isp is 58.4 sec, and the arm length around the z axis is 100 mm, the required fuel for two years to manage the angular momentum is calculated as 0.1 kg. Therefore, the fuel amount is confirmed to be sufficient.

**Table 4: ADCS specification.**

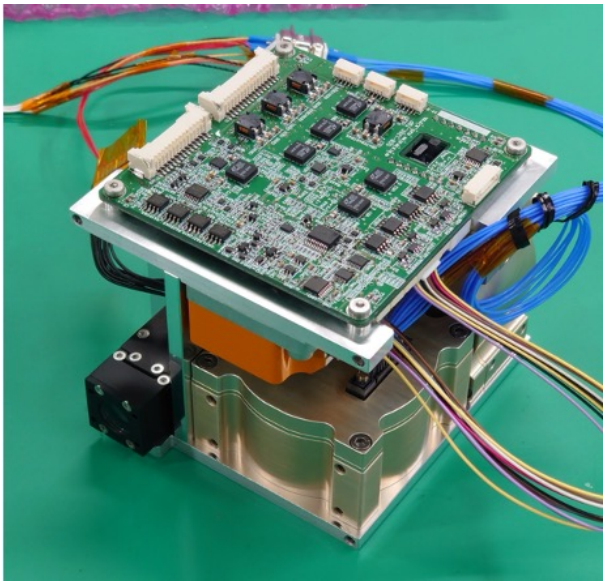

**Figure 8: Engineering model of the ADCS module.**

### *Power*

The solar array panel (SAP) has a cell string configuration of 7-series/6-parallel on the front side and 7-series/4-parallel on the back side. After SAP deployment, the maximum power generation when directly facing the Sun is 50.8 W. The battery consists of lithium-ion cells arranged in a 3-series/2-parallel configuration, with a capacity of 77.7 Wh. During steady-state operations, the power consumption is

20.6W, and power analysis results confirmed that the power balance is adequately maintained.

The average power generation in a tumbling state is 12.2W. Even if the satellite enters a tumbling state, power consumption can be reduced to 9.83W by turning off the attitude control system components and reducing the XTRP transmission duty cycle to 1/6. By entering this safe mode, it was confirmed that the power balance is maintained, ensuring operational sustainability even with a loss of attitude control.

### *Telecommunication*

The telecommunication system of the LunaCube mainly consists of a legacy XTRP from the EQUULEUS mission,[31] two Rx low gain antennas (Rx-LGA), four Tx low gain antennas (Tx-LGA), one middle gain antenna (Tx-MGA), hybrids (HYB), and RF switches, which are connected as shown in Figure 9. Rx-LGAs are installed on ± Z, and any attitude assure at least 256 bps according to link budget analysis. Tx-LGAs are installed on ± X and ± Z. Each pair is combined through a HYB, and it is switched through an RF switch.

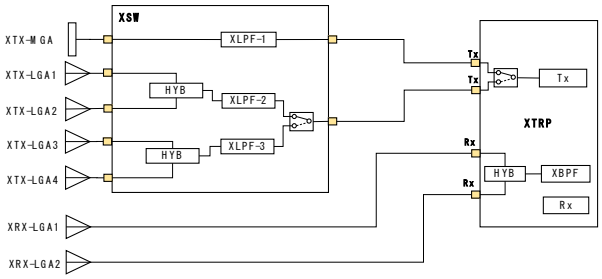


**Figure 9: Telecommunication system diagram.**

### *Thermal*

Numerical simulations for steady and transition states are conducted to analyze thermal conditions. In lunar orbits, the angle between the Sun's direction and the orbital plane $\beta$ changes gradually due to perturbations, affecting the satellite's exposure to the Moon's infrared radiation. Thermal analysis has revealed that the satellite's temperature decreases as the solar angle $\beta$ approaches 90 degrees and increases as it approaches 0 degrees. Based on the variations in distance between the Sun and the satellite and the lunar surface environment, the possible values for the solar constant and albedo are determined. Then, the worst-case high temperature condition was defined as a solar angle $\beta$ of 0 degrees, a solar constant of 1421 W/m$^2$, and an albedo of 0.2. The worst-case low temperature condition was defined as a solar angle $\beta$ of 90 degrees, a solar constant of 1315 W/m$^2$, and an albedo of 0.07. In both scenarios, it was confirmed that all components are maintained within the acceptable temperature range.

Temperature transitions during lunar eclipses have also been calculated. During a lunar eclipse, assumed to last 5 hours, the temperature of each component drops to approximately -10 degrees Celsius as shown in Figure 10. However, all components were confirmed to remain within their acceptable temperature ranges.

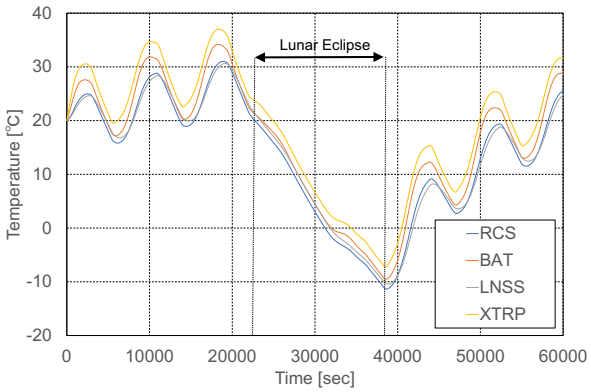


**Figure 10: Temperature transitions during 5 hours lunar eclipse.**

### *System Integration*

The integration of engineering model was completed as shown in Figure 11.

**Figure 11: The integration of the engineering model.**

Thermal vacuum testing of the engineering model was conducted, as shown in Figure 12. The

results of operational tests at a low temperature of -10°C and a high temperature of +50°C confirmed the integrity of the satellite engineering model under thermal vacuum conditions.

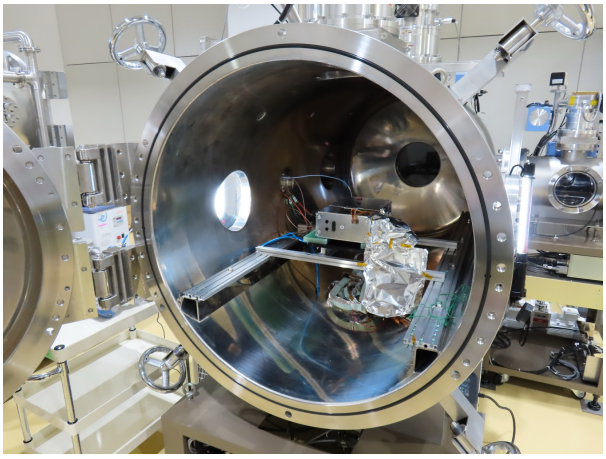

**Figure 12: The configuration of thermal vacuum testing.**

Vibration testing of the engineering model was also conducted, as shown in Figure 13. The results confirmed that there are no issues with the engineering model's design.

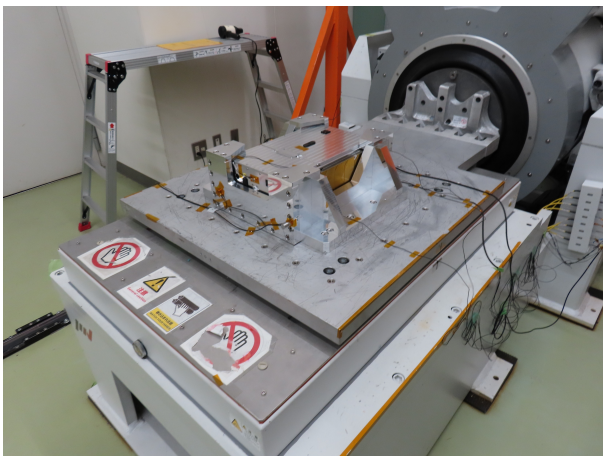

**Figure 13: The configuration of thermal vacuum testing.**

## CONCLUSION

This paper presents the mission design of 6U dual-satellite lunar navigation and communication system, LunaCube. The orbit selection showed that the navigation accuracy and orbit maintenance cost requirement is satisfied with low lunar orbits. The system design confirmed that each subsystem satisfies requirements to provide lunar navigation and communication service in low lunar orbits. In addition, this paper presents the engineering model development results. They cinfirmed the functionality of the system in cislunar environments.

LunaCube has progressed through preliminary design in 2021, detailed design in 2022, and the development of an engineering model in 2023. LunaCube is currently exploring rocket launch options to lunar orbit as it transitions to the development of the flight model.

## References


[1] David J Israel, Kendall D Mauldin, Christopher J Roberts, Jason W Mitchell, Antti A Pulkkinen, D Cooper La Vida, Michael A Johnson, Steven D Christe, and Cheryl J Gramling. Lunanet: a flexible and extensible lunar exploration communications and navigation infrastructure. In *2020 IEEE Aerospace Conference*, pages 1–14. IEEE, 2020.

[2] Pietro Giordano, Floor Malman, Richard Swinden, Paolo Zoccarato, and Javier Ventura-Traveset. The lunar pathfinder PNT experiment and moonlight navigation service: The future of lunar position, navigation and timing. In *Proceedings of the 2022 International Technical Meeting of The Institute of Navigation*, pages 632–642, 2022.

[3] Masaya Murata, Masaru Koga, Yu Nakajima, Ryoichiro Yasumitsu, Tomohiro Araki, Katsumi Makino, Kyohei Akiyama, Toru Yamamoto, Kota Tanabe, Satoshi Kogure, et al. Lunar navigation satellite system: mission, system overview, and demonstration. In *39th International Communications Satellite Systems Conference (ICSSC 2022)*, volume 2022, pages 12–15. IET, 2022.

[4] Toshiki Tanaka, Takuji Ebinuma, Shinichi Nakasuka, Takeshi Matsumoto, Rion Sobukawa, and Yoshihide Aoyanagi. Systems design results of lunacube: Dual-satellite lunar navigation system with 6u-cubesats. *Acta Astronautica*, 216:318–329, 2024.

[5] Toshiki Tanaka, Takuji Ebinuma, and Shinichi Nakasuka. Dual-satellite lunar global navigation system using multi-epoch double-differenced pseudorange observations. *Aerospace*, 7(9):122, 2020.

[6] Wu Shilong, Luo Jingqing, and Gong Liangliang. Joint fdoa and tdoa location algorithm

and performance analysis of dual-satellite formations. In *2010 2nd international conference on signal processing systems*, volume 2, pages V2–339. IEEE, 2010.

[7] William Jun, Kar-Ming Cheung, Julia Milton, Charles Lee, and Glenn Lightsey. Autonomous navigation for crewed lunar missions with dban. In *2020 IEEE Aerospace Conference*, pages 1–13. IEEE, 2020.

[8] William W Jun, Kar-Ming Cheung, E Glenn Lightsey, and Charles Lee. Localizing in urban canyons using joint doppler and ranging and the law of cosines method. In *Proceedings of the 32nd International Technical Meeting of the Satellite Division of The Institute of Navigation (ION GNSS+ 2019)*, pages 140–153, 2019.

[9] Michael Music, Lesley Newberry, David Peters, Gregory Quetin, Angela Stickle, Ken Ackerman, Erik Bruun, Tyler Cleveland, Thomas Culver, Joni Deboever, Raymond Do, Joseph Grant, Ladonna Hanugan, Greg Haselfeld, Matt Heikell, John Mayberry, John Robbins, Alec Sabin, Derek Schmuland, and Ryan Trescott. Luna polaris a lunar positioning and communications system. 12 2022.

[10] Christian Circi, Daniele Romagnoli, and Federico Fumenti. Halo orbit dynamics and properties for a lunar global positioning system design. *Monthly Notices of the Royal Astronomical Society*, 442(4):3511–3527, 2014.

[11] K Iiyama. Optimization of navigation satellite constellation and lunar monitoring station arrangement for lunar global navigation satellite system (lgnss). In *Proceedings of the 32nd International Symposium on Space Technology and Science (ISTS), Fukui, Japan*, pages 15–21, 2019.

[12] Mattia Carosi, Jacopo Capolicchio, Massimiliano Tosti, Massimo Eleuteri, Cosimo Stallo, Daniele Musacchio, and Carmine Di Lauro. Comparison among orbital constellations for a global lunar satellite navigation system. 09 2021.

[13] Hongru Chen, Lei Liu, Yazhe Meng, Zhenyu Xu, Long Long, and Jiangkai Liu. Preliminary mission design and analysis of a lunar far-side positioning cubesat mission. In *26th International Symposium on Space Flight Dynamics. Matsuyama, Japan, paper ISTS–2017–d–160/ISSFD–2017–160*, 2017.

[14] Zhao-Yang Gao and Xi-Yun Hou. Coverage analysis of lunar communication/navigation constellations based on halo orbits and distant retrograde orbits. *The Journal of Navigation*, 73(4):932–952, 2020.

[15] Yuan Ren and Jinjun Shan. Libration point orbits for lunar global positioning systems. *Advances in Space Research*, 51(7):1065–1079, 2013.

[16] Miriam Schonfeldt, Antoine Grenier, Anaïs Delépaut, Pietro Giordano, Richard Swinden, Javier Ventura-Traveset, Daniel Blonski, and Jörg Hahn. A system study about a lunar navigation satellite transmitter system. In *2020 European Navigation Conference (ENC)*, pages 1–10, 2020.

[17] Filipe Pereira and Daniel Selva. Exploring the design space of lunar gnss in frozen orbit conditions. In *2020 IEEE/ION Position, Location and Navigation Symposium (PLANS)*, pages 444–451. IEEE, 2020.

[18] Gheorghe Sirbu, Mauro Leonardi, Mattia Carosi, Carmine Di Lauro, and Cosimo Stallo. Performance evaluation of a lunar navigation system exploiting four satellites in elfo orbits. In *2022 IEEE 9th International Workshop on Metrology for AeroSpace (MetroAeroSpace)*, pages 146–151. IEEE, 2022.

[19] M Shirobokov, S Tromov, and M Ovchinnikov. Lunar frozen orbits for small satellite communication/navigation constellations. In *Proceedings of the International Astronautical Congress, IAC*, 2021.

[20] Obed S Sands, Joseph W Connolly, Bryan W Welch, James R Carpenter, Todd A Ely, and Kevin Berry. Dilution of precision-based lunar navigation assessment for dynamic position fixing. In *Proceedings of the 2006 National Technical Meeting of The Institute of Navigation*, pages 260–268, 2006.

[21] Angel David Arcia Gil, Daniel Renwick, Chantal Cappelletti, and Paul Blunt. Methodology for optimizing a constellation of a lunar global navigation system with a multi-objective optimization algorithm. *Acta Astronautica*, 204:348–357, 2023.

[22] Filipe Pereira and Daniel Selva. Analysis of navigation performance with lunar gnss evolution. In *Proceedings of the 2022 International*

*Technical Meeting of The Institute of Navigation*, pages 514–529, 2022.

[23] A Batista, E Gomez, H Qiao, and KE Schubert. Constellation design of a lunar global positioning system using cubesats and chip-scale atomic clocks. In *Proceedings of the International Conference on Embedded Systems and Applications (ESA)*, pages 1–4, 2012.

[24] Mick Wijnen, Nereida Agüera-Lopez, Sara Correyero-Plaza, and Daniel Perez-Grande. Cubesat lunar positioning system enabled by novel on-board electric propulsion. *IEEE Transactions on Plasma Science*, 46(2):319–329, 2018.

[25] Shuichi Matsumoto, Mina Ogawa, Yasuhiro Kawakatsu, Hisahiro Konishi, Hitoshi Ikeda, Hiroshi Terada, Kimie Tanaka, Takaaki Kato, K. Otani, Erika Kamikawa, and Shingo Ikegami. Flight results of selenological and engineering explorer "kaguya" on lunar orbit. 2009.

[26] Mark Beckman and Rivers Lamb. Stationkeeping for the lunar reconnaissance orbiter (lro). 2007.

[27] Diane C Davis and Ryan J Whitley. Enhanced stationkeeping maneuver control technique for delta-v cost reduction in the korea pathfinder lunar orbiter. In *AAS Astrodynamics Specialists Conference*, number JSC-E-DAA-TN60023, 2018.

[28] P Wolff, F Pinto, B Williams, and R Vaughan. Navigation considerations for low-thrust planetary missions. 1998.

[29] Erwan Mazarico, DD Rowlands, GA Neumann, DE Smith, MH Torrence, FG Lemoine, and MT Zuber. Orbit determination of the lunar reconnaissance orbiter. *Journal of Geodesy*, 86(3):193–207, 2012.

[30] Jun Asakawa, Hiroyuki Koizumi, Keita Nishii, Naoki Takeda, Masaya Murohara, Ryu Funase, and Kimiya Komurasaki. Fundamental ground experiment of a water resistojet propulsion system: Aquarius installed on a 6u cubesat: Equuleus. *Transactions of the Japan Society for Aeronautical and Space Sciences, Aerospace Technology Japan*, 16(5):427–431, 2018.

[31] Ryu Funase, Satoshi Ikari, Kota Miyoshi, Yosuke Kawabata, Shintaro Nakajima, Shunichiro Nomura, Nobuhiro Funabiki, Akihiro Ishikawa, Kota Kakihara, Shuhei Matsushita, et al. Mission to earth–moon lagrange point by a 6u cubesat: Equuleus. *IEEE Aerospace and Electronic Systems Magazine*, 35(3):30–44, 2020.